




Sterane and hopane biomarkers capture microbial transformations of complex hydrocarbons in young hydrothermal Guaymas Basin sediments

Paraskevi Mara ^{1,4}, Robert K. Nelson^{2,4}, Christopher M. Reddy², Andreas Teske ³ & Virginia P. Edgcomb ¹✉

In Guaymas Basin, organic-rich hydrothermal sediments produce complex hydrocarbon mixtures including saturated, aromatic and alkylated aromatic compounds. We examined sediments from push cores from Guaymas sites with distinct temperature and geochemistry profiles to gain a better understanding on abiotic and biological hydrocarbon alteration. Here we provide evidence for biodegradation of hopanoids, producing saturated hydrocarbons like drimane and homodrimane as intermediate products. These sesquiterpene by-products are present throughout cooler sediments, but their relative abundance is drastically reduced within hotter hydrothermal sediments, likely due to hydrothermal mobilization. Within the sterane pool we detect a trend toward aromatization of steroidal compounds within hotter sediments. The changes in hopane and sterane biomarker composition at different sites reflect temperature-related differences in geochemical and microbial hydrocarbon alterations. In contrast to traditionally observed microbial biodegradation patterns that may extend over hundreds of meters in subsurface oil reservoirs, Guaymas Basin shows highly compressed changes in surficial sediments.

¹Department of Geology and Geophysics, Woods Hole Oceanographic Institution, Woods Hole, MA, USA. ²Department of Marine Chemistry and Geochemistry, Woods Hole Oceanographic Institution, Woods Hole, MA, USA. ³Department of Earth, Marine, and Environmental Sciences, University of North Carolina, Chapel Hill, Chapel Hill, NC, USA. ⁴These authors contributed equally: Paraskevi Mara, Robert K. Nelson. ✉email: vedgcomb@whoi.edu

The Guaymas Basin is an active oceanic spreading center in the central Gulf of California, covered by several hundred meters of organic-rich hemipelagic sediments (Supplementary Fig. S1 panel A). Shallow magmatic sill intrusions transform sedimentary organic matter—primarily planktonic and microbial detritus—into thermal degradation and alteration products such as CH₄, CO₂, ammonia, short-chain aromatic acids, alkanes, and aromatic hydrocarbons^{1–5}. Shallow sill emplacement moves the thermal window of petroleum generation into recently deposited sediments where fresh photosynthetic biomass is transformed into young hydrocarbons that subsequently migrate to the sediment surface, as indicated by the young ¹⁴C radiocarbon age (approximately 5000–6000 years) for hydrocarbons collected in the hydrothermally active southern axial trough of Guaymas Basin⁶. Hydrothermal fluids carrying complex mixtures of hydrocarbons⁷ create an extensive mosaic of hydrothermal sediment habitats, including mounds and microbial mats⁸, and sustain diverse and active microbial communities^{9–11}.

Hydrothermal pyrolysis of organic carbon is well documented not only in surficial sediments but also in deep Guaymas Basin sediments and deeply buried sills. The organic carbon content of ~3–4 wt% in surficial Guaymas Basin sediments¹² is reduced to 1–2% in deep (tens to hundreds of meters below seafloor (mbsf)) subsurface sediments^{13,14}, and to <1% at the sediment–sill interface in a well-studied, currently deeply buried off-axis sill between 350 and 430 m depth¹⁵. Current in situ temperatures at this off-axis sill are in the range of 80–100 °C¹⁵ but were likely higher at the time of sill emplacement. Thus, the available evidence from surficial and deep subsurface sediments indicates that the transformation of sedimentary organic matter into hydrocarbons is a persistent and widespread process in Guaymas Basin that, depending on the hydrothermal setting, occurs on different spatial scales.

Recently, high-resolution bathymetric surveys combined with shallow sub-bottom seismic profiles penetrating ca. 30–60 m below the sediment surface have shed new light on hydrocarbon formation, mobilization, and seepage in the southern axial trough of Guaymas Basin¹⁶. In small seafloor depressions where massive subsurface hydrothermal precipitates have formed and lithified, hydrothermal fluids follow relatively shallow and convoluted flow paths that skirt surface-breaching hydrothermal edifices. Soluble and volatile light hydrocarbons such as C₁–C₁₀ gases, oil, and condensates, are transported by hydrothermal fluids towards shallow sediments where they accumulate^{16,17}. These flows account for frequent observations of hydrothermal hot spots and microbial mats at the base or along the lower slopes of hydrothermal mounds¹⁸. This setting has produced a vast patchwork of hydrothermal sediments, microbial mats, and hot hydrocarbon seeps in the southern axial trough that is frequently sampled during microbiological and biogeochemical surveys (e.g. refs. ^{8,15}, and this study).

Compound-specific chromatographic analysis of hydrocarbons can be used to identify microbial biomarkers (compounds either of biological origin or derived from biological decomposition of parent compounds) and their degradation products, and thus provide a foundation for understanding the imprint of biological hydrocarbon alteration in a deep-sea hydrocarbon seep sediments. The molecular transformations of hydrocarbons in sediments exposed to a range of temperatures (0–155 °C) were recently investigated in shallow push cores collected from the Cathedral Hill site in Guaymas Basin using comprehensive two-dimensional gas chromatography (GC×GC) and chemometrics¹⁷. The analyses of these surficial sediments (0–20 cm depth) yielded highly complex hydrocarbon mixtures and revealed downcore hydrocarbon compositional changes attributed to hydrocarbon

migration and water-washing of hydrocarbons that become solubilized due to increasing hydrothermal activity and circulation. As heat-driven fluids flow upward through the sediments, the mobilizable fraction of organic matter, including hydrocarbons that may otherwise be condensed onto cold particle surfaces, can be captured by these flows due to thermal cleavage of molecular bonds or poly-condensation reactions for polyaromatic hydrocarbons¹⁷. Decreased diversity and concentration of alkylated aromatic hydrocarbons as well as unsubstituted polyaromatic hydrocarbons in deeper, hotter, layers of push cores were observed, and steroid and hopanoid biomarkers showed distinguishable patterns and down-core concentration variability due to the combined effect of hydrocarbon migration and solubilization¹⁷. Steroids are components of cell membranes in plants, animals, and fungi, and serve as biological signaling molecules, and hopanoids are triterpenoids found in membranes of bacteria, some land plants, and fungi, and include simple hopenes, hopanoids, and hopanes, and their functional derivatives. Here we expand on this work by investigating the potential for microbial degradation of biomarkers in surficial sediments (up to 40 cmbsf) with microbially compatible temperatures, using gas chromatography analyses (e.g., GC-FID, GC-MS) and GC×GC to identify the inventories of hydrocarbons and biomarkers present at different sites and sediment depths. We focus especially on hopane and sterane molecules that occur abundantly in surficial Guaymas Basin sediments¹⁹, and on their biodegradation intermediates. Microbial utilization/breakdown of such compounds has been suggested for Guaymas Basin (e.g. ref. ²⁰) but has so far not been specifically investigated. Such activities of microorganisms would contribute to the complex carbon pools available under the sulfidic and anoxic conditions of these hydrothermal sediments. They also may provide sensitive bioindicators for the early stages of microbial diagenesis in organic-rich hydrothermal sediments.

Results and discussion

Sampling sites and temperature gradients for hydrothermal sediment. Guaymas Basin sites were visited and sampled with R/V *Atlantis*, HOV *Alvin*, and AUV *Sentry* during cruise AT42-05 (November 15–29, 2018). *Alvin* dives targeted previously surveyed sampling areas of the Southern Guaymas trough with hydrothermal sediments and microbial mats in the Cathedral Hill, Aceto Balsamico, and Marker 14 sampling areas, plus a background site (Table 1, Supplementary Fig. S1 panel A). These sampling sites have been described previously^{8,21}.

Spots with different combinations of mat cover and thermal regime were selected for push core sampling. Sediments without microbial mats have cool temperatures throughout (core 4991–35, and background core 4999–8). The sediments of the Aceto Balsamico area are temperate and reach ca. 20 °C at 45 cm depth (cores 4992–24, 4998–20). Most hydrothermal cores of the Cathedral Hill area were obtained from warm sediments (ca. 30–50 °C at 45 cm depth), whereas the Marker 14 core 4998–15 and Cathedral Hill core 5000–8 were collected from hot sediments that reach ca. 80 °C at 20 cm or >115 °C at 30 cm depth (Table 2, Supplementary Fig. S1). Photo coverage of *Alvin* dives is available at the *Alvin* frame-grabber site [<http://4dgeo.who.edu/Alvin>].

GC×GC hydrocarbon pool analyses at different Guaymas sites and sediment depths. The Alpha Analytical GC-FID and GC-MS results provided information on broad hydrocarbon profiles for cores from all study sites and showed consistent evidence for the effect of hydrothermal activity that concentrates hydrocarbons differently in surficial sediments due to the distinct in situ temperatures (see below, Alpha Analytical methods²², and Supplementary

Table 1 Guaymas hydrothermal sediment sampling locations.

Dive & core no.	Sampling area	Lat/Long	Depth (m)	Microbial Mat cover	Sectioning intervals (cm)	Sample type(s)	Thermal regime at deepest sample
4991-7	Cathedral Hill (CH)	27.0114/111.4045	2014	Orange	0-6, 6-12, 12-18	*Sediment & porewater	Warm, 37 °C
4991-35	Cathedral Hill (CH)	27.0114/111.4045	2014	Bare sediment	0-10,10-20, 20-30	Sediment & porewater	Cool, 14 °C
4991-41	Cathedral Hill (CH)	27.0114/111.4045	2014	White/orange	0-10,10-20, 20-30	Porewater	Warm, 31 °C
4992-24	Aceto Balsamico (AB)	27.0081/111.4071	2012	Yellow	0-10, 10-20	Porewater	Temperate, 20 °C
4994-5	Cathedral Hill (CH)	27.0114/111.4045	2014	Orange	0-7, 7-14, 14-21	Porewater	Warm, ~48 °C
4998-15	Marker 14	27.0079/111.4072	2011	Orange	0-7, 7-14, 14-21	*Sediment & porewater	Hot, >115 °C
4998-20	Aceto Balsamico (AB)	27.0078/111.4071	2011	Yellow	0-10,10-20, 20-30	Sediment & porewater	Temperate, 22 °C
4999-8	Background	27.0069/111.4066	2014	Bare sediment	0-7, 7-14, 14-21	Porewater	Cool, 4 °C
5000-8	Cathedral Hill (CH)	27.0122/111.4039	2009	Orange	0-7, 7-14, 14-21	Porewater	Hot, ~80 °C

The sediment characteristics and sampling schemes are presented for cores that were used for hydrocarbon analyses at Alpha Analytical (GC-FID and GC-MS analyses). Asterisk shows the six sediment cakes analyzed with GC×GC at WHOI.

Discussion). The quantitative results and compound classes of hydrocarbons identified in the sediment cakes and porewaters are reported in Supplementary Data 1 and 2.

Sediments from temperate core 4991-7 from the Cathedral Hill area (30 °C at 20 cmbsf) and hot core 4998-15 from the Marker 14 area (>100 °C at 30 cmbsf) showed strongly contrasting hydrocarbon distribution (Fig. 1) and alteration within the top ~15 cm sediment (Fig. 2, Supplementary Data 1) and were selected for GC×GC analyses to gain more finely resolved information on the compounds present. GC×GC hydrocarbon analysis allowed us to investigate further the role of hydrocarbon mobilization in Guaymas sediments, but also search for evidence of microbial hydrocarbon biodegradation and evaluate biomarker potential²³ at these two geochemically/thermally distinct Guaymas Basin sites.

In the surface layer of temperate core 4991-7 from Cathedral Hill, GC×GC analysis of extractable material indicated abundant PAHs that are preferentially accumulated at the surface over lighter and more volatile C₁–C₁₀ hydrocarbons, and diverse and abundant molecules such as sesquiterpanes, hopanes, steranes, di- and triaromatic steroids, and tetraaromatic hopanoids (Fig. 3). These abundant compounds are consistent with the rapid transformation of marine sedimentary biomass of planktonic origin to petroleum hydrocarbons under local sedimentary seafloor temperature gradients²⁴. GC×GC analysis also identified organosulfur hydrocarbons including benzothiophenes, dibenzothiophenes, and benzonaphthothiophenes, as well as phenanthrothiophenes, chrysenothiophenes and dinaphthothiophenes (Supplementary Fig. S2; Supplementary Table S3). The sulfur-containing PAHs (PASHs) were enriched in higher molecular weight multi-ring aromatics and were depleted in the low molecular weight range of the GC×GC-HRT chromatogram, indicating that the lighter and more volatile PASH compounds formed in the surficial Guaymas sediments migrate rapidly out of the sediments, similar to the lighter and volatile PAHs.

The role of temperature and hydrothermal activity in mobilizing hydrocarbons is illustrated by a side-by-side comparison of GC×GC-FID chromatograms for the temperate core 4991-7 from Cathedral Hill and the hotter core 4998-15 from the Marker 14 sampling area (Fig. 2; see also the GC×GC *peak subtraction analyses* section below). Both cores show a broad spectrum of hydrocarbons from alkanes toward increasingly oxidized and aromaticized compounds (Supplementary Fig. S3). The temperate core 4991-7 from Cathedral Hill contains a more complex milieu of hydrocarbons than the hot core 4998-15 from Marker 14, indicating greater hydrocarbon accumulation under more moderate hydrothermal temperature conditions. In temperate core 4991-7 from Cathedral Hill, all sediment layers analyzed (0–6, 6–12, 12–18 cmbsf, corresponding to ~0–5, ~5–14, and ~14–21 °C, respectively) are rich in hydrocarbons, in contrast to hotter Marker 14 core 4998-15, where hydrocarbon abundance is strongly skewed toward the upper sediment layers (0–7 and 7–14 cmbsf), and appears much reduced at depth (14–21 cmbsf, corresponding to ~52–74 °C). This distinct downcore profile suggests that hydrocarbons at the hotter Marker 14 site are mobilized to a greater extent by the higher temperatures and flushed towards the sediment surface by rising hydrothermal fluids. The steep thermal gradient at this site reaches ca. 75 °C at 20 cm depth and >115 °C at 40 cm depth (Table 1) and is one of the hottest hydrothermal sites sampled during the 2018 expedition²¹. In contrast, the more temperate conditions at Cathedral Hill (4991-7; ca. 30 °C at 20 cm, and 37 °C at 40 cm depth, Supplementary Fig. S1) indicate lower hydrothermal activity which favors hydrocarbon retention and accumulation.

Table 2 Temperature profiles for Guaymas sediment cores.

Depth (cm)	4991-7 (T°C)	4991-35 (T°C)	4991-41 (T°C)	4992-24 (T°C)	4994-5* (T°C)	4998-15 (T°C)	4998-20 (T°C)	4999-8 (T°C)	5000-8 (T°C)
0	-	3.4-5.4	3.4-4.4	3-3.6	-	-	3-3.5	3.2	-
5	3.3-4.8	4.6	7.9	5.7	5	12.4	5	-	20.6/23/33
10	8.9	6.7	9.3	7.3	10.4	33.3	7.3	-	44/53/69
15	16.7	8	11.6	9.2	-	53.7	8.6	-	-
20	24.1	9	14	11	-	74.1	10.7	-	74/80/86
25	30.7	10.6	17.2	12.7	26	92.2	12.5	-	-
30	31.9	12.1	20.3	14.4	-	110.4	14.8	-	-
35	35.8	13.1	23.4	16.0	-	112.4	17.3	-	-
40	36.7	13.7	26.8	17.8	-	>115	19.5	-	-
45	37.1	13.7	31	19.7	48	>115	21.7	3.9	-

Note the inherent variability in some sampling areas. Core 4998-15 (Marker 14) was collected near two applicable thermal profiles T1 (shown here) and T2 that showed consistent results; in both cases, the thermal sensors of the heat-flow probe reached their limit below 35 cm depth. In contrast, thermal profiles measured near core 4991-7 (Cathedral Hill) vary considerably over short distances, from ca. 13 °C at 50 cm just outside the hydrothermal mat area to 80 °C at 50 cm further into the hydrothermal area (not shown).

*T°C profile for 4994-5 was taken at a nearby mat area, but not adjacent to this core.

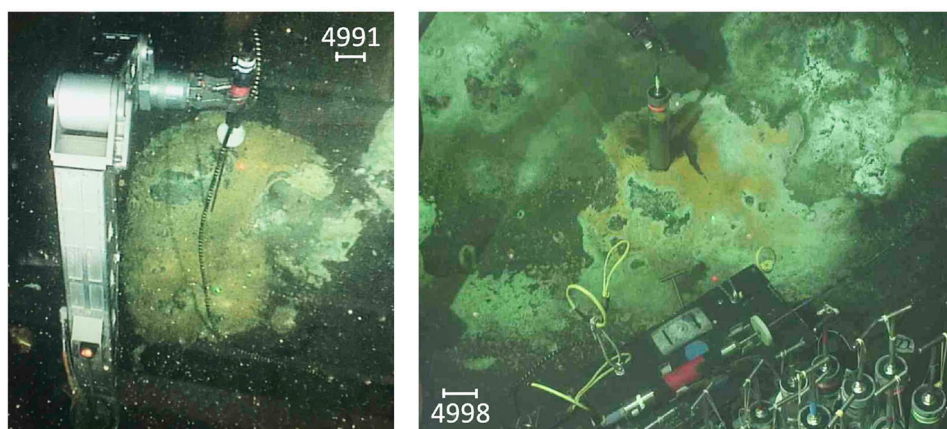


Fig. 1 Hydrothermal sediment sampling sites for cores 4991-7 (Cathedral Hill) and 4998-15 (Marker 14 area). The Cathedral Hill site (4991) and Marker 14 (4998) sites are covered with white, yellow and orange mats of sulfur-oxidizing bacterial mats (*Beggiatoaceae*). The two sites differ by temperature gradient. Scale bars are 10 cm based on *Alvin*'s laser beam scaler and the diameter of *Alvin* pushcores. Courtesy of Andreas Teske, U. North Carolina, Chapel Hill/NSF/AUV *Sentry*/2016 ©Woods Hole Oceanographic Institution.

GC×GC peak subtraction analyses in different sediment layers.

We used subtraction analyses to explore compound-specific compositional differences across the entire GC-amenable hydrocarbon spectrum in multiple sediment horizons collected from the temperate Cathedral Hill (4991-7) and hot Marker 14 (4998-15) cores. The high reproducibility and resolution provided by GC×GC-FID analysis allows for matching the two-dimensional (2D) chromatograms of the different sediment layers, and tracking the gradual downcore changes by peak subtraction (Fig. 4). In this approach, the GC×GC chromatograms from the different sediment layers are subtracted from each other to comprehensively capture the differences in peak abundance and distribution (e.g. refs. 17,23,25). These analyses showed that the temperate core 4991-7, contains a complex pool of saturated, cyclic to fully polycyclic aromatic hydrocarbons which appear enriched in the surface layer, whereas a subset of this pool (mostly alkylbenzenes, naphthalenes, and fluorenes) is found predominantly in the deeper region of the core (Fig. 4a). Saturated hydrocarbons with low linear (*n*)-alkane carbon numbers (C₉-C₁₆), and recalcitrant compounds with higher *n*-alkane carbon numbers (C > 16), such as pristane and phytane, appear predominantly in deeper layers of our cores. In contrast to temperate core 4991-7, analysis of the hot core 4998-15 shows that almost the entire pool of hydrocarbons is enriched in the

surface layer. Only a few peaks in the fringe of alkylbenzenes, naphthalenes, and fluorenes with reduced *n*-alkane numbers remain slightly enriched in the subsurface, indicating near-complete hydrothermal mobilization towards the surface of 4998-15 (Fig. 4b). Interestingly, saturated hydrocarbons with low *n*-alkane numbers remain relatively enriched in the subsurface, reflecting possibly selective alkane migration and loss at the sediment surface of 4998-15, or microbial alkane degradation in the surface sediments by sulfate-reducing alkane-oxidizing bacteria and archaea²⁶. Finally, subsurface alkanes might also represent residuals from demethylation or cyclization reactions that are affecting a wide range of hydrocarbons.

Comparison of the Guaymas Basin hydrocarbons with reference materials.

The petroleum mixtures of surficial Guaymas Basin hydrothermal sediments are distinct from crude oil standards and from refined oils, as they contain a broad and highly complex spectrum of increasingly aromaticized compounds (UCM, unresolved complex mixture²⁷) that contrasts with individually separated peaks for alkylated benzenes, naphthalenes, fluorenes, phenanthrenes, and pyrenes that dominate in the crude and refined oil references (Fig. 2, Supplementary Fig. S4). The complex petroleum mixtures of surficial Guaymas Basin hydrocarbons suggest the impact of oxidative weathering and microbial

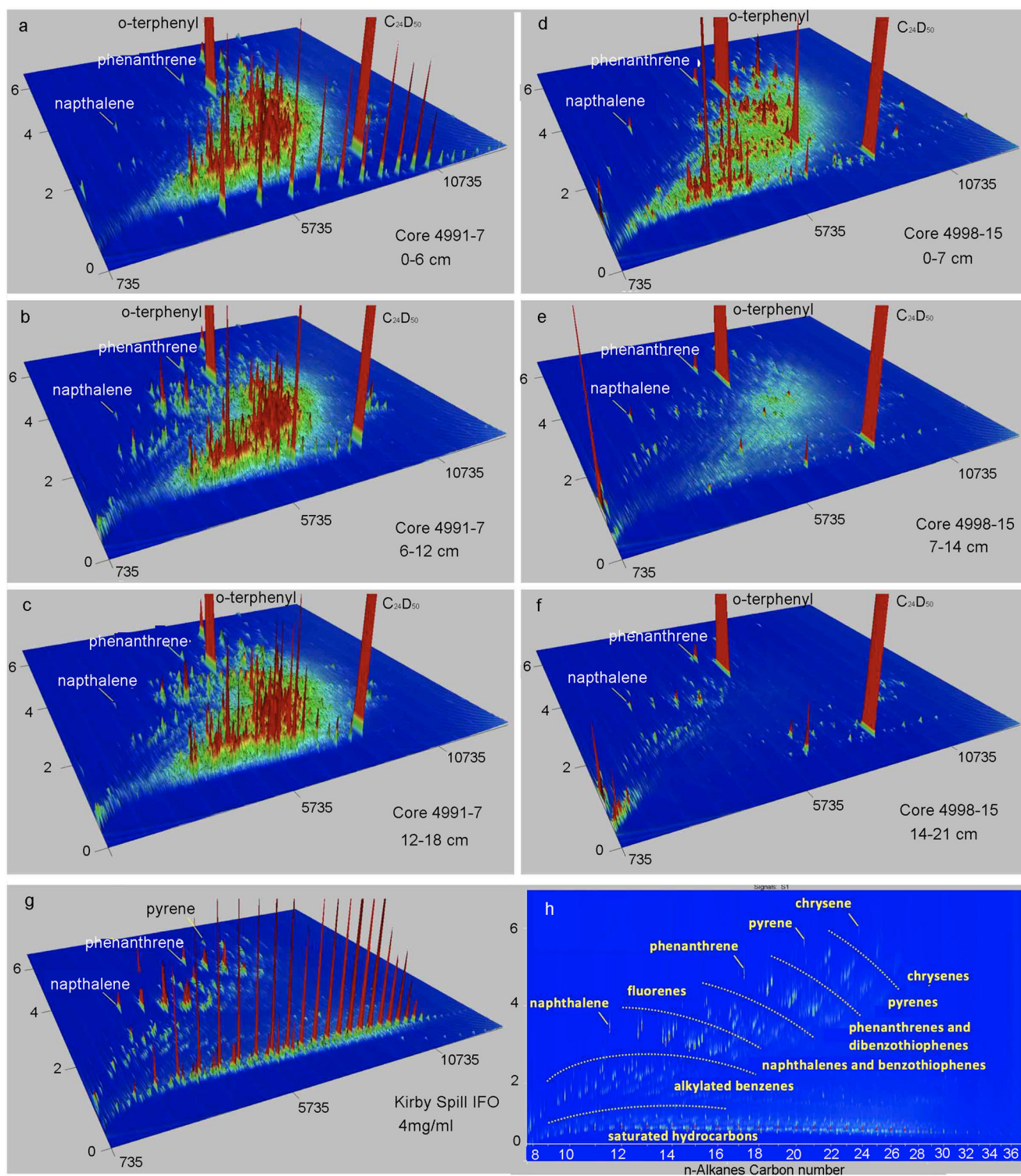


Fig. 2 GC×GC-HRT mountain plot of solvent extractable hydrocarbons from contrasting Guaymas cores. Temperate core 4991-7 is from Cathedral Hill (A-C, corresponding to -0-5, -5-14, and -14-21 °C, respectively), hot core 4998-15 is from Marker 14 (D-F, corresponding to 0--20 °C, -20-52 °C, and -52-74 °C, respectively). **a** GC×GC-HRT mountain plot compares solvent extractable hydrocarbons from temperate core 4991-7 (mountain plots **a-c**) and hot core 4998-15 (mountain plots **d-f**). An annotated sample of intermediate fuel oil (IFO) is shown as a mountain plot in panel (**g**) and the data is presented in plan view in panel **h** highlighting the elution fairways of saturated hydrocarbons, alkylated benzenes, naphthalenes and benzothiophenes, fluorenes, phenanthrenes and dibenzothiophenes, pyrenes, and chrysenes. GC×GC-FID versions of chromatograms from core 4991-7 and core 4998-15 are shown in Supplementary Fig. S3. The large peaks in chromatograms **a-f** are *o*-terphenyl and perdeuterated tetracosane internal standards added during the sample preparation.

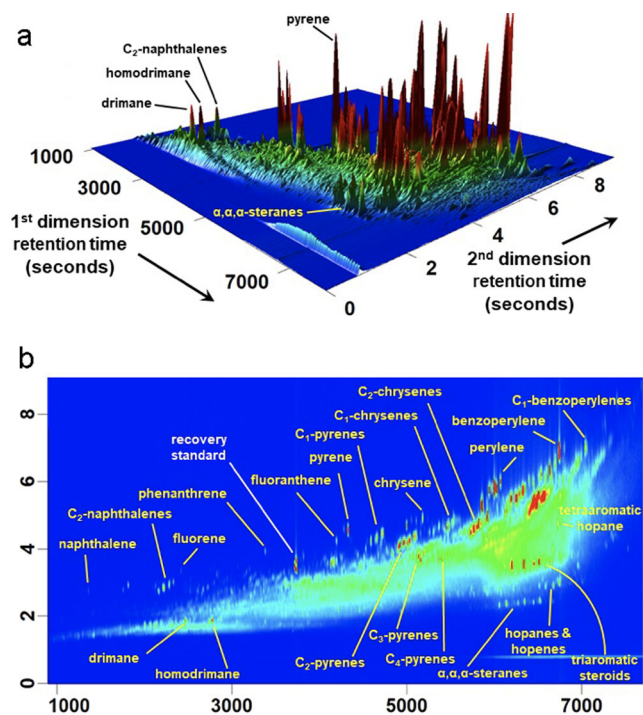


Fig. 3 Solvent extractable material from Cathedral Hill Sediment core 4991-7. The 0–6 cm section, is shown as a 3D GC×GC-HRT mountain plot (a) and as color contour plot of the same GC×GC-HRT chromatogram (b). Annotated peaks include polynuclear aromatic hydrocarbon (PAHs) compounds as well as sesquiterpanes, hopanes, steranes, di- and triaromatic steroids, and tetraaromatic hopanoids.

degradation on surficial sediments where hydrothermal circulation introduces seawater and electron acceptors⁸.

Distribution of biomarkers in Guaymas Basin sediments. The GC×GC profiles for Guaymas Basin core 4991-7 and 4998-15 show the consistent occurrence of biomarkers, including eukaryotic steranes/diasteranes, monoaromatic and triaromatic steroids, and bacterial hopanes/hopenes (Supplementary Fig. S5). Steranes have important roles in membrane rigidification, energy budgeting, and pigmentation; in marine ecosystems, they are derived mainly from phytoplankton (e.g., diatoms/dinoflagellates), terrestrial plants, or higher eukaryotes deposited into oxidizing environments²⁸. Hopanes are predominately compounds of bacterial origin²⁸, suggesting that the hopanoid pool detected in these hydrothermal sediments derives mostly from benthic bacteria that are active during the early stages of diagenesis, and respond to the availability of organic carbon and hydrothermal energy sources²⁹. Additionally, some hopanes may derive from detrital phytoplankton from the overlying water column, however numerous sequencing surveys of Guaymas Basin sediments have detected very few cyanobacterial marker genes^{18,19,21}, and cyanobacteria are therefore likely to only be minor contributors to the hopane pool.

The molecular transformations of steroid and hopanoid biomarkers in Guaymas Basin sediments can be attributed to two major pathways (Fig. 5): one involves chemical transformations of steranes and hopanes via oxidation reactions which are promoted by the hydrothermal environment of Guaymas Basin (Fig. 5, red arrows), while the other pathway reflects their microbial degradation (blue arrows). Abiotic transformations result in aromatized hopanoid and steroid compounds. In contrast, the microbial biodegradation pathways convert hopanoids to 8,14-secohopanoid and further to sesquiterpenoids,

yielding compounds composed of the A and B rings of the parent hopanoid, namely, drimane and homodrimane, both detected in Guaymas Basin sediments. We trace these proposed pathways below by documenting the abundance and distribution of sterane, hopanoid and sesquiterpenoid compound in the Guaymas sediment cores.

Steranes in Guaymas sediments and their biodegradation.

Sterane compounds are more dominant and occur in all layers in the cooler temperate core 4991-7, and are less conspicuous in hot core 4998-15, where they disappear from its bottom layer (Supplementary Fig. S5). Diasteranes, products of sterane diagenesis (Supplementary Fig. S6) that accumulate in oils from mature sediments and clastic source rocks²⁸, become more prominent towards the bottom of core 4991-7 (Supplementary Fig. S5). The milder in situ temperatures in core 4991-7 (ca. 20–30 °C, below the oil window of 60–70 °C) argue against an in situ origin of these diasteranes as thermal rearrangement products. Unless the mobility of these diasteranes allows them to be introduced upward from deeper and hotter sediments, they might represent products of biological sterane degradation. However, it should be noted that precursor sterols are transformed via a complex network that involves biogenesis, diagenesis, and catagenesis, and is also affected by the maturity of the sediment²⁸.

A GC×GC-HRT chromatogram that includes sterane compounds and their degradation products shows the difference in sterane content between Cathedral Hill (4991-7) and Marker 14 (4998-15) sampling sites. Sterane compounds decreased gradually downcore in the temperate core 4991-7, and more rapidly in the hot core 4998-15, where only traces of steranes remained at depth (Supplementary Figs. S7 and S8). We detected the aromatization of steroidal compounds at both Marker 14 and Cathedral Hill sites. Abundant triaromatic steroidal compounds were present in all of the sediment horizons analyzed from Cathedral Hill and also in surficial sediments (0–7 cm) from Marker 14 (Supplementary Fig. S7). Monoaromatic steranes, the proximate product of sterane aromatization²⁸, increase with depth in temperate core 4991-7, but are barely detectable in hot core 4998-15 (Supplementary Fig. S7). The next products in the aromatization sequence, triaromatic steranes, are the most abundant sterane form in temperate core 4991-7 and almost the only sterane form observed in hot core 4998-15 (Supplementary Fig. S7). This rapid change from non-aromatic to mono- and triaromatic steranes within ca. 20 cm of a steep downcore thermal gradient indicates the rapid thermal maturation and defunctionalization of planktonic steranes to polycyclic aromatic hydrocarbons in Guaymas Basin sediments. These observations are also consistent with oxidizing conditions in the surficial sediments, due to seawater mixing by hydrothermal circulation⁸.

With increasing temperature, triaromatic steroid compounds undergo catagenetic alterations that cause complete aromatization and cracking and are expected to be completely transformed into more stable aromatic hydrocarbons (e.g., substituted phenanthrenes³⁰). Degradation products of triaromatic steranes, monoaromatic steranes, and steranes, all missing their alkyl side chains, appear prominently throughout the temperate core 4991-7 (Supplementary Fig. 8A–C). In the surface sample of core 4998-15, these degradation products overshadow their source compounds, and they recede to trace levels below the surface sediment (Supplementary Fig. 8D–F). This strongly skewed distribution and abundance pattern in hot core 4998-15, and the much more gradual concentration changes of these degradation products in the temperate core 4991-7, suggest different degrees of hydrothermal mobilization and concentration towards surficial sediments.

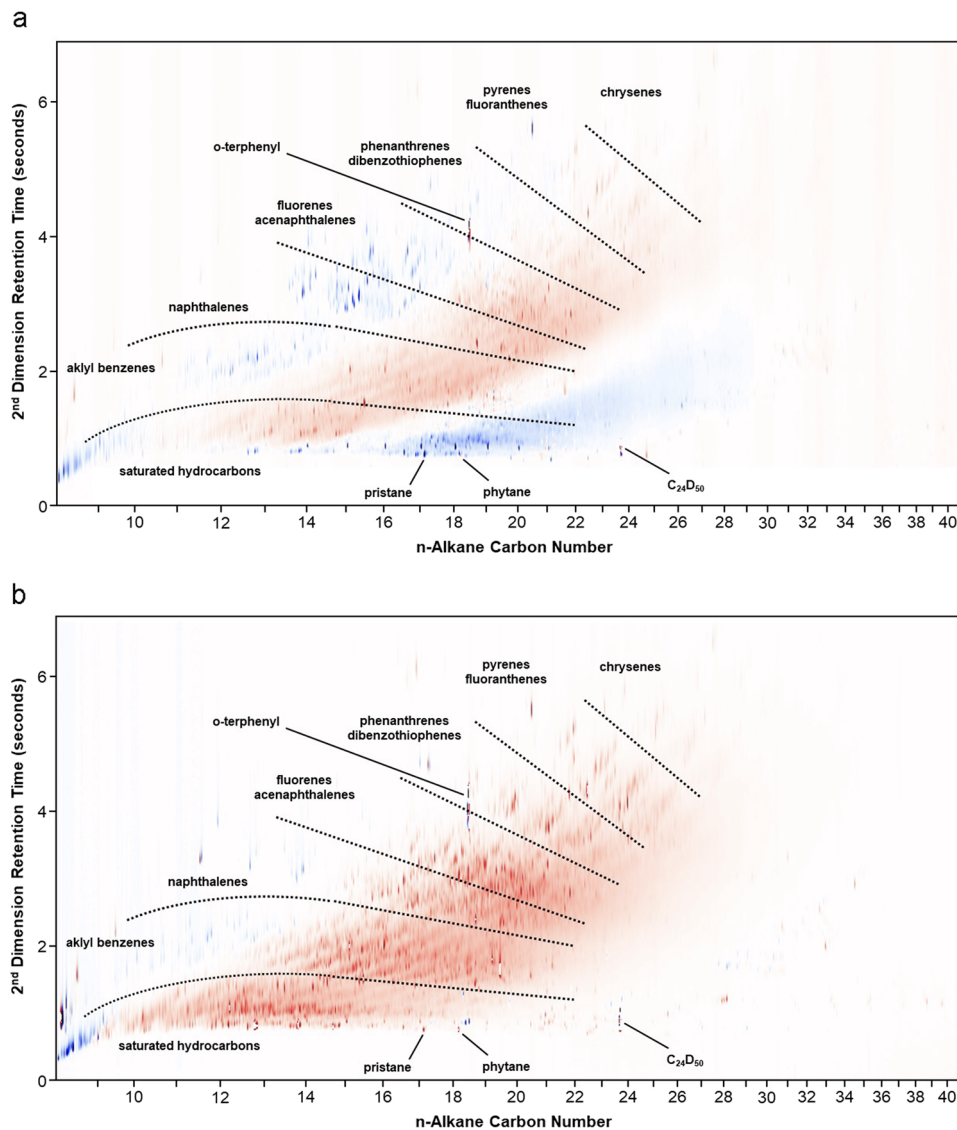


Fig. 4 Difference chromatograms for Guaymas Basin sediment cores. These chromatograms compare the presence and relative abundance of hydrocarbons in the core top compared to about mid-level in the core. The Cathedral Hill core 4991-7 (**a**) compares the 0–6 and 12–18 cm depth intervals. The Marker 14 core 4998-15 (**b**) hydrocarbons in the 0–7 and 14–21 cmbsf depth intervals. Compounds that remain at the same abundance throughout the core vanish in the subtraction chromatogram (cancellation). Red peaks highlight compounds with positive values. In these chromatograms, lower core depth (12–18 and 14–21 cmbsf) intervals were subtracted from the 0–7 cmbsf interval. Red peaks represent hydrocarbons that are more abundant in the 0–7 cmbsf interval. Conversely, blue peaks represent negative values and indicate greater relative abundance in the deeper depth interval. In sum, red peaks indicate compounds present in higher abundance in the surficial depth interval, and blue peaks are those more abundant down core.

Sources of steranes in Guaymas Basin sediments. Since steroidal compounds in petroleum commonly originate from plant/phytoplankton biomass, we considered whether the steroidal compounds in Guaymas Basin sediments represent biogenic sedimentation in this highly productive region of the Gulf of California³¹. The spectrum of steranes in our sediment samples includes unsubstituted (C_{27}), methylated (C_{28}), ethylated (C_{29}), and in smaller amounts, propylated steranes (C_{30}), with short alkane substitutions consistently occurring at C_{24} as confirmed by mass spectrometric reconstruction of specific sterane peaks (Supplementary Fig. S9). Close inspection of the detected steranes and diasteranes highlighted a suite of steranes with unique proton orientations on the molecule and fragment ion masses. Steranes with protons at positions 5, 14, and 17 all in the alpha orientation (below the rings) of the sterane molecule (abbreviated α,α,α) produce a unique fragment ion with a mass of 217.1951 amu (Fig. 6, Supplementary Fig. S9), and are considered to be typical

of early diagenesis³². As diagenesis progresses, new sterane isomers are formed that have greater thermal stability³². These new sterane isomers have protons at positions 5, 14, and 17 in the alpha, beta, beta (α,β,β) configuration and produce a unique fragment ion with a mass of 218.2029 amu. These isomers were not observed in any of the investigated Guaymas Basin core samples, indicating that the α,β,β configuration, which is formed as the level of thermal maturity increases, has not yet occurred. Thus, the identified steroidal compounds in these sediments are in the very early stages of diagenesis, consistent with high rates of biogenic sedimentation that ensure a steady supply of fresh phytoplankton biomass.

The GC×GC analysis of sediment samples from both Marker 14 and Cathedral Hill also revealed the presence of sterols in surficial sediments. Sterols are a subgroup of steroids essential to cell membranes for maintaining their microfluid state³³. Although various sterol biosynthetic enzymes can function under

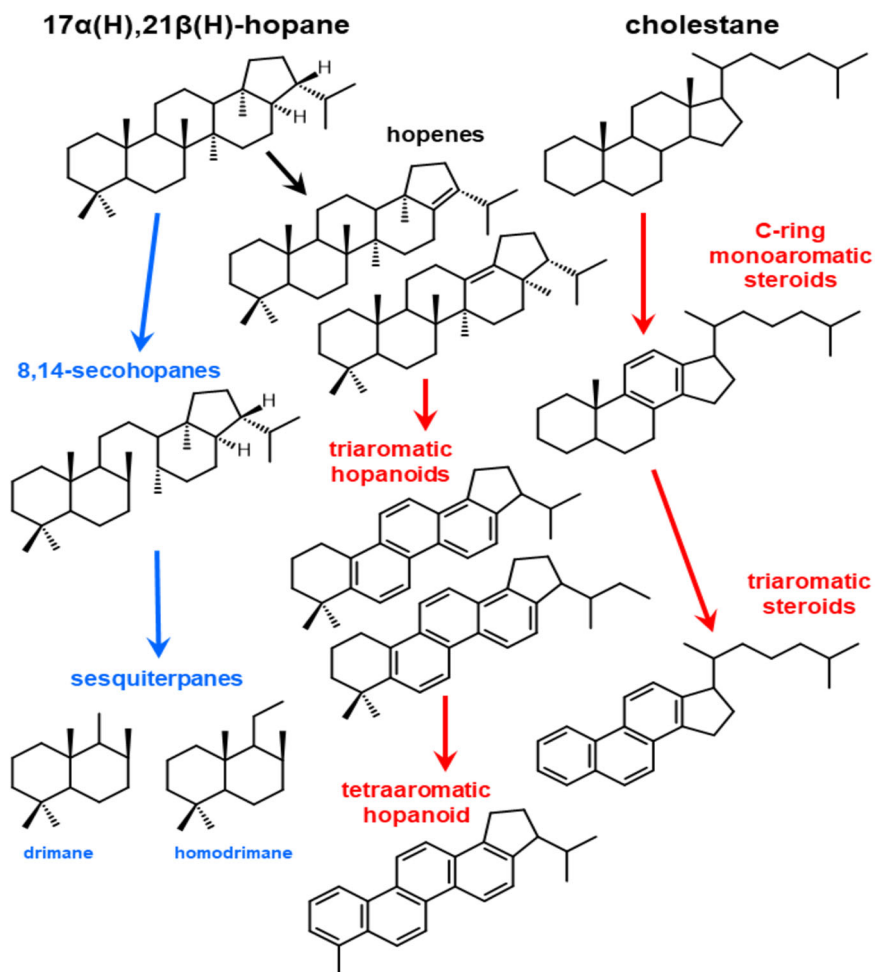


Fig. 5 Overview of hopane and sterane biodegradation and oxidation pathways in Guaymas Basin organic-rich sediments. The molecules 17 α (H),21 β (H)-hopane and cholestane were used as model compounds. Blue arrows indicate microbial biodegradation transforming hopanoids to sesquiterpanes, and red arrows indicate abiotic oxidation to form aromatized hopanoid and steroid compounds.

extremely low oxygen conditions³⁴, sterol biosynthesis requires molecular oxygen. Under anoxic conditions, sterols are neither produced nor easily scavenged/acquired from the environment via transporters³⁵. Thus, sterols in anoxic Guaymas Basin sediments are almost certainly derived from phytoplankton, especially diatoms and diverse green algae originating from the highly productive upper water column of Guaymas Basin^{31,36}. Diatom-derived sediments are extensive in the Gulf of California, particularly in the deep, central part of Guaymas Basin where we sampled³⁷. The high dissolved silica content of Guaymas sediments and the conspicuous silica enrichment (mostly amorphous opal) in Guaymas hydrothermal structures indicate that diatoms undergo hydrothermal alterations to siliceous hydrothermal deposits³⁸. Laboratory experiments using hydrothermal liquefaction to convert wet biomass of diatoms/microalgae into liquid fuel have identified various derivatives including sterols as major biocrude constituents³⁹. Under slow or fast pyrolysis the pyrolytic oil fraction of diatoms and microalgae exhibits a wide variety of C₁₅–C₃₀ alkenes/alkane amides, terpenes, and pyrrolidines⁴⁰.

Similar results to those reported during pyrolysis and hydrothermal liquefaction of diatoms were found for pyrolysis of C₂₇–C₂₉ sterols in green algae and chlorophyta⁴¹. Pyrolysis yielded a wide range of C₃₀ sterane compounds, indicating that C₂₉ sterols that predominate in green algae can generate C₃₀ steranes within sediments through diagenetic methylation⁴¹.

Confined pyrolysis of Guaymas sediments generated C₂₇ to C₂₉ steranes, confirming rapid reduction of microalgal sterols, while extensive pyrolysis (>24 h) caused isomerization of the steranes resulting in a pattern representative of a fully mature oil⁴².

Aromatic steranes in Guaymas Basin and the Uzon caldera.

The coexistence of steranes with their aromatic analogs (e.g., mono- and triaromatic steranes) in a hydrothermal sulfur-rich sediment gradient motivated a search for comparable samples and their potential transformation pathways. The triaromatic steranes in young Guaymas Basin hydrocarbons (ca. 5000 years old by radiocarbon dating; ref. 6) resembled those of young oil collected from Uzon caldera (Kamchatka) that are ¹⁴C-dated to ca. 4000 years (provided by Allen Marshall and Ryan Rogers, National High Magnetic Field Laboratory, Tallahassee, FSU). The GC–MS results from the Uzon caldera oils revealed that steranes and hopanes are dominant components existing at approximately equal proportions in the Uzon hydrocarbon pool, with hopane biomarkers deriving from bacterial precursor molecules⁴³. The steroid hydrocarbons encompassed a mixture of C₂₇–C₂₉ $\alpha\alpha\alpha$ -steranes and C₂₇–C₂₈ normethyl triaromatic steranes, while the hopanes ranged from C₂₇ to C₃₅ hopanes (no C₂₈) and included 17 α (H),21 β (H) configurations⁴³. The shared occurrence of triaromatic steranes in young, hot oil from this surficial volcanic site and from deep-sea hydrothermal sediments suggests a formation pathway that operates only under specific conditions,

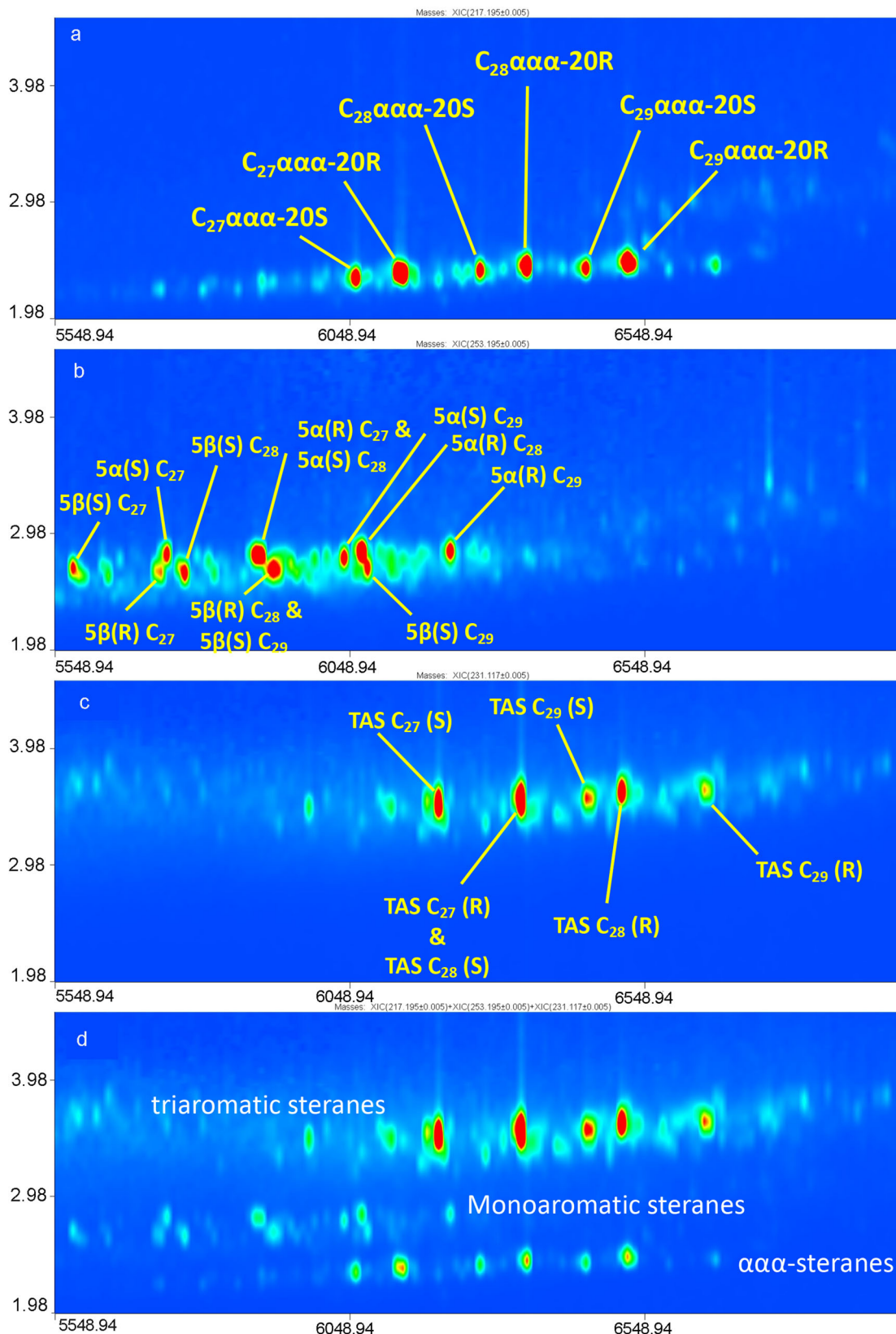


Fig. 6 GC×GC-HRT color contour plot of Cathedral Hill core 4991-7 (0–6 cm) which highlights the aromatization pathways of $\alpha\alpha$ -steranes. **a** Shows aromatization of the $\alpha\alpha$ -steranes, **b** shows resulting C-ring monoaromatic steroidal compounds, and **c** shows resulting triaromatic steroidal compounds. **d** Shows all compounds in overview. $\alpha\beta$ -steranes were not observed. Selected ions, m/z 217.195 (**a**), 253.195 (**b**), 231.117 (**c**), all ± 0.005 amu.

potentially at both near-surface atmospheric exposure and in the deep sea under oxidizing conditions that occur with seawater inmixing by hydrothermal circulation/alteration⁸. In both environments, triaromatic steranes are unlikely to be retained long-term. We speculate that due to the volcanic or hydrothermal heat at both sites (Uzon caldera and Guaymas Basin), the accumulating deposition-derived sterane signal is more widely detectable in the upper sediment than the bacterial hopanoid pool that represents indigenous bacterial communities inhabiting the relatively narrow habitable zone in hot sediment.

Hopanes in Guaymas sediments and their degradation products. Bacterial hopanes are environmentally recalcitrant⁴⁴ and preserve their stereochemical configuration throughout early diagenesis and even thermal maturation. Analogous to steranes, confined pyrolysis experiments of Guaymas sediments under anaerobic conditions yielded C₂₇–C₃₀ hopanes that occurred in their fully mature 17 α (H),21 β 3(H)-configurations, which are usually present in naturally altered sediments⁴². Yet, hopanes can be degraded under specific conditions, and these Guaymas Basin sediments provide a case study for hopane degradation products and potential microbial degradation pathways that complement aerobic processes⁴⁵.

Consistent with their recalcitrance, hopanes, benzohopanes, and presumably biological demethylation products (25-nor-terpenoids⁴⁶), occur more abundantly in hot core 4998-15 than in temperate core 4991-7 (Supplementary Fig. S5). Hopanes are degraded via the cleavage of the hopane ring into 8,14 secohopanes (Fig. 5) which accumulate in highly biodegraded oils, indicative of a microbial process⁴⁷. Microbial diagenesis then generates the sesquiterpanes drimane and homodrimane, that occur widely in petroleum source rocks, crude oil, and sediments⁴⁸. Drimane and homodrimane are detectable by GC×GC-HRT in all layers of temperate core 4991-7 and in the two upper layers of hot core 4998-15 (Supplementary Fig. S10). Supplementary Fig. S10 highlights a region of the GC×GC chromatogram that captures the elution of sesquiterpanes (drimane and homodrimane). Supplementary Fig. S11 reveals sesquiterpanes (with the m/z 123.117 amu ion) as well as the hopanoid suite of compounds (with the m/z 191.179 amu ion). Figure S11 also shows that drimane and homodrimane are highly abundant compounds, and panel B shows that a peak labeled “I” is 17 α ,21 β (H)-hopane (the mass spectra of peaks A, B, and I can be found in Supplemental Fig. S12). Following the possible molecular transformation scenario presented in Fig. 5 (blue arrows), the sesquiterpanoids are derived from hopanoid precursor molecules. It is, therefore most reasonable that the abundant Guaymas sesquiterpanoids resulted from the transformation of hopanoids. Guaymas Basin sediments thus show clear evidence of microbially catalyzed hopane degradation. This microbial breakdown of hopane could contribute to the carbon pools available under the sulfidic and anoxic conditions occurring in the Guaymas Basin hydrothermally distinct sediments.

The presence of aromatized steroidal compounds in this study prompted us also to search for aromatized hopanoid compounds that could be formed in Guaymas Basin sediments due to oxidizing conditions in surficial sediments. We find evidence that hopanes and hopenes are oxidized to form aromatized hopanoids (Fig. 7, Supplementary Figs. S11 and S12), and in particular, we note the presence of B, C, D-ring triaromatic hopanoids and an A, B, C, D-ring tetraaromatic hopanoid compound that could be produced by abiotic oxidation (red arrows in Fig. 5). A comparable suite of triaromatic hopanoids was described in Ordovician Kukersite shales, as well as an oxidative pathway that starts at the D-ring of hopanoid molecules and advances to the C-

ring, to the B-ring, and finally to the A-ring⁴⁹ (see also Supplementary Discussion). Our GC×GC data show the same oxidative pathway is likely to be present in Guaymas Basin sediments. We also identified triaromatic homohopanooid (peak M) and triaromatic bishomohopanooid (peak N) compounds (Fig. 7, Supplementary Figs. S11 and S12). Finally, oxygen-containing hopanes also occur in Guaymas Basin sediments. A high-resolution mass spectral profile of a suite of oxygen-containing hopenoids in the Guaymas Basin sediments (peaks O, R, and S; Fig. 7, Supplementary Figs. S12 and S13) shows the potential incorporation of an oxygen hetero-atom into the E-ring of hopene molecules (see Supplementary Discussion for details). Comparable 17(21)-hopenes (without oxygen hetero-atoms) were identified previously in biomass of the sulfur-oxidizing photoheterotrophic bacterium *Rhodospseudomonas palustris*⁵⁰, consistent with sulfur-rich conditions and the abundance of sulfur-oxidizing bacteria in surficial hydrothermal sediments of Guaymas Basin⁸.

Hopanoids were suggested to be incorporated into cell membranes for maintaining cell wall stability in anaerobic fungi like *Neocallimastigomycota*^{35,51}. Fossil fungal hyphae samples from fractured bedrock contained a quite significant number of hopanoids ranging from C₂₇ to C₃₅, but no steranes (35). Since Guaymas sediments harbor diverse fungal phyla including zoospore fungi (e.g. *Chytridiomycota*) and *Neocallimastigomycota* (21), it remains to be investigated whether *Neocallimastigomycota* and/or other fungal phyla utilize hopanoids to substitute for sterols under anoxic and sulfidic conditions, or whether novel hopanoids are part of their membrane mosaic.

Conclusions

Within the top centimeters of hydrothermal sediment in Guaymas Basin, biological compounds experience rapid alteration. The fate of planktonic steranes includes the diagenetic rearrangement to diasteranes, rapid α,α,α to α,β,β isomerization, and downcore aromatization to monoaromatic and triaromatic compounds. Bacterial hopanes are degraded by demethylation at position C-25 to produce 25-nor-hopanoids⁴⁶, by cleavage of the hopane ring structure into sesquiterpanes, by oxidation to tri- and tetraaromatic hopanoids, and by insertion of heteroatomic oxygen into hopenes. The sulfur-rich conditions in Guaymas Basin hydrothermal sediments allow for the production of abundant organosulfur hydrocarbons. The changes we observed in hopane and sterane biomarker composition in cores that we analyzed are consistent with high levels of biodegradation in Guaymas Basin surficial sediments^{52,53}. While these changes in biomarker composition are observed in both of the contrasting cores analyzed with GC×GC analysis, they show a vertically extended distribution in temperate sediments (Cathedral Hill; core 4991-7), whereas in hot sediments these molecules occur near the sediment surface and rapidly disappear below the surface (Marker 14; core 4998-15). This distribution pattern is likely evidence of hydrocarbon migration and washing of lighter hydrocarbons that solubilize due to increasing hydrothermal activity (Fig. 8). In hot, highly active hydrothermal sediments, the entire suite of source compounds and alteration products is shifted upwards and appears concentrated in surficial sediments because they are likely flushed from deeper layers. Such a process constitutes a compound-specific analog to hydrothermal flushing of sedimentary organic matter, as found in previous studies of Guaymas Basin sediments⁵⁴.

Rapid concentration changes that reflect the mobilizing impact of hydrothermalism on hydrocarbon distribution have been noted previously. Decreasing downcore hydrocarbon distributions were previously observed²⁷ in two Guaymas Basin cores

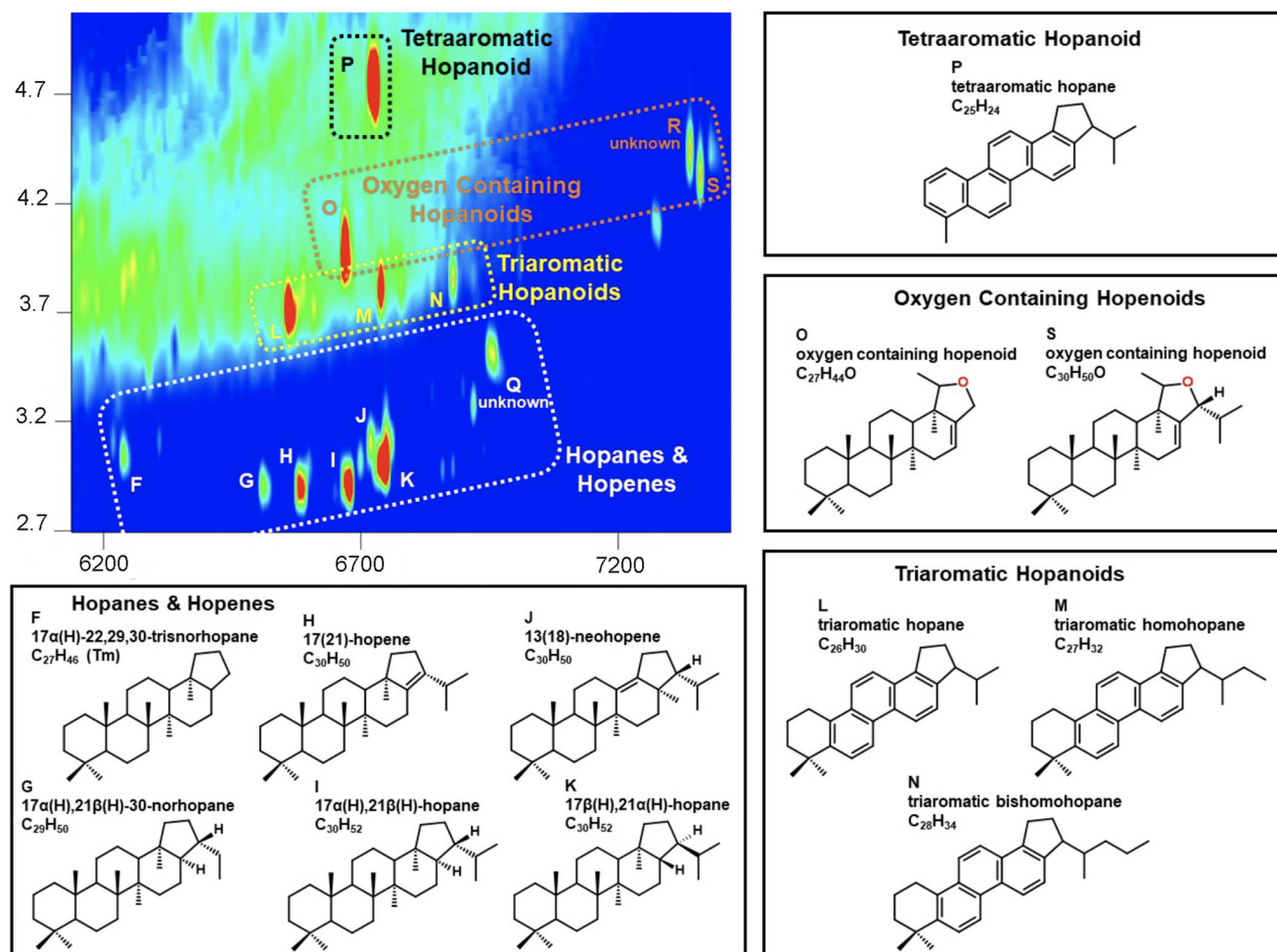


Fig. 7 GC×GC-HRT color contour plot of Cathedral Hill core 4991-7 (0–6 cm) highlighting hopane degradation and oxidation products, using selected ions (m/z 123.117, 191.179, 257.132, 281.133, 324.187, 410.391, and 412.406 all ± 0.005 amu). Peak assignments start at F to correlate with Supplementary Fig. S11 panel b. Peaks F, G, I, and K are the hopanoids 17 α (H)-22,29,30-trisnorhopane, 17 α (H)-30-norhopane, 17 α (H),21 β (H)-hopane, and 17 β (H),21 α (H)-hopane (aka moretane), respectively. Peaks H, J, and Q are the hopenes identified as 17(21)-hopene, 13(18)-neohopene, and an unknown hopene, respectively. Peaks L, M, and N are triaromatic hopane, triaromatic homohopane, and triaromatic bishomohopane, respectively. Peaks O, R, and S are hopanoids that contain an oxygen hetero atom, and peak P is a tetraaromatic hopanoid.

with contrasting thermal regimes (temperate core 1611 with 46 °C at 24 cm depth, and hot core 1615 with 120–130 °C at 20–30 cm depth), indicating that hydrothermal activity generally results in hydrocarbon mobilization from deeper high-temperature sediments, and retention and accumulation in temperate surficial sediments. Yet, the same hydrothermal factors that concentrate hydrocarbons and biomarkers towards the sediment surface impact the distribution, abundance, and activities of microorganisms in Guaymas Basin sediments, with the result that microbial activity in hotter Guaymas Basin sediments is most concentrated in surficial sediments within approx. 5 cm. The in situ temperature profiles and the availability of diverse carbon/nutrient sources all shape microbial community structure and activity. Surficial hydrothermal sediments of Guaymas Basin exhibit maxima in sulfate reduction⁵⁵ and acetate oxidation rates⁵⁶, rapid consumption of oxygen and nitrate⁵⁷, and microbial population maxima, reflected in cell counts⁵⁸, microbial lipid concentrations^{59,60}, DNA concentrations⁶¹ and in serial dilutions of cultivable heterotrophic thermophiles⁶². These consistent trends of near-surface maximum microbial density and activity indicate that microbial hydrocarbon and biomarker degradation would occur predominantly in surficial sediments where they can compete most effectively with abiotic processes, and where

temperatures are not inhibiting microbial growth and/or activity. Consistent with this notion, the surficial sediments of Guaymas Basin continue to generate discoveries of unusual hydrocarbon-degrading bacteria and archaea (e.g. ref. ⁶³), and they provide an attractive model system for exploring the microbial mechanisms, pathways and agents of hydrocarbon degradation in compound- and microbe-specific detail.

Methods

Temperature survey and sampling procedure. Microbial mat-covered hydrothermal sediments were thermally profiled using *Alvin's* 50 cm heat flow probe (<https://ndsf.whoi.edu/alvin/using-alvin/sampling-equipment/>). The 50 cm probe contains five thermal sensors every 10 cm, starting 5 cm under the attached plastic disk (the “puck”) that limits probe penetration and rests on the seafloor once the probe is fully inserted. Temperature is measured in two steps, first with the puck 5 cm above the seafloor, and then on the seafloor, resulting in a 5 cm resolution. After ~3–5 min, temperature readings stabilized and were recorded within *Alvin*.

Push cores of 30–40 cm in length were returned to the surface after each *Alvin* dive, and within a few hours sampled in the shipboard laboratory for porewater and solid phase geochemistry²¹. Sediment cores were divided into three depth horizons of 6–10 cm thickness, depending on individual core lengths. ~40 ml subsamples of each depth horizon were aliquoted into two sterile 50 ml Falcon tubes and were immediately centrifuged at 3000 rpm for 15 min to separate porewater from sediment cakes. After centrifugation, the porewaters were carefully collected using a 60 ml sterile syringe and filtered through a 0.45 μ m cellulose filter (Millipore, USA). Porewater samples of ~20 ml were collected into gas-tight serum

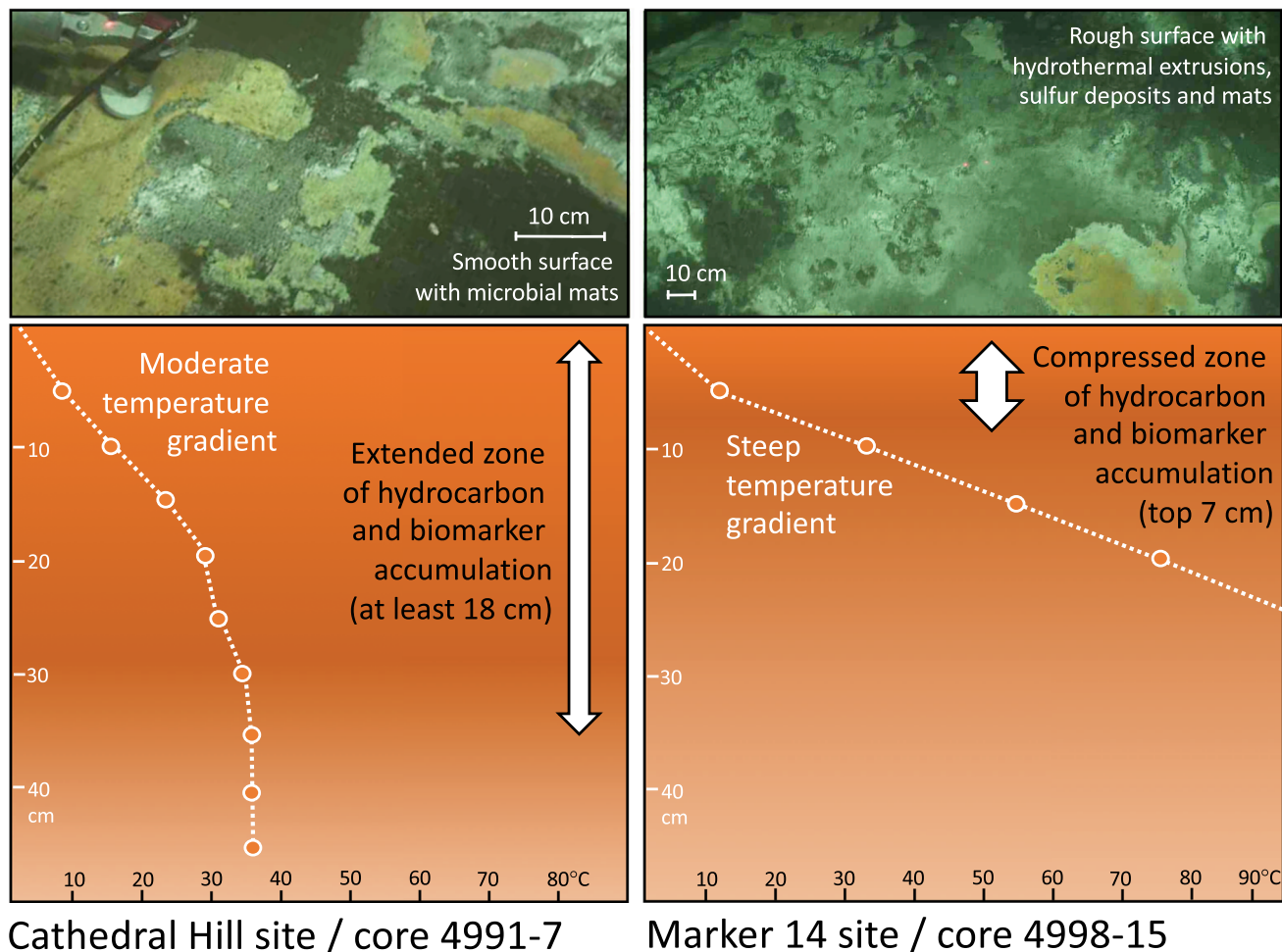


Fig. 8 Overview of contrasting thermal regimes at Cathedral Hill and Marker 14 sites in Guaymas Basin. At Cathedral Hill, moderate temperature gradients extend the zone of hydrocarbon and biomarker accumulation deeper into the sediments than at hotter Marker 14, where steep temperature gradients compress the zone of hydrocarbon and biomarker accumulation into the top ~7 cmbsf.

vials sealed with black stoppers and crimp seal and stored at 4 °C. The sediment cakes from each horizon were kept in 50 mL Falcon tubes and stored at 4 °C until hydrocarbon analysis.

Sediment and porewater geochemistry. Geochemical analyses were performed on centrifuged porewaters and sediments from three layers per core at the LSU Wetland Biogeochemistry Analytical Services center. Alvin pushcores were sectioned to recover the 0–6, 6–12, and 12–18 cm fractions, or the 0–10, 10–20, and 20–30 cm fractions, depending on core recovery. Colorimetric determinations of ammonium, nitrate, soluble reactive phosphorus and total phosphorus were performed using an OI Analytical Flow Solutions IV auto analyzer. Total nitrogen and carbon (wt%) are measured with a Costech 1040 CHNOS Elemental Combustion system. Filtered porewater samples were analyzed for dissolved organic carbon (DOC) and total dissolved nitrogen (TDN) using a Shimadzu TOC/TN analyzer. Dissolved organic nitrogen (DON) was calculated by subtracting TDN from the sum of the inorganic nitrogen species. The data are tabulated in Supplementary Table S1.

Gas phase analysis of saturated and polynuclear aromatic hydrocarbons. 26 porewater and 12 sediment cake samples from cores collected at Cathedral Hill, Aceto Balsamico, and Marker 14 sampling areas were submitted for hydrocarbon analyses (Table 1; Supplementary Data 1, 2, Supplementary Table 2, Supplementary Data 3, 4). Each sample was analyzed for traditional fingerprinting diagnostic compounds, (e.g., saturated hydrocarbons, polynuclear aromatic hydrocarbons (PAHs), alkylated PAHs) by Alpha Analytical using United States Environmental Protection Agency (EPA) method 8015 (GC-FID; saturates) and a modified method 8270D (GCMS; PAHs). Methods and performance details are provided in ref. 22.

Two-dimensional gas chromatography (GC×GC)

GC×GC-FID analyses: Highly resolved GC×GC FID chromatographic analyses were performed as described previously (17) using a LECO system consisting of an

Agilent 7890A GC configured with a split/splitless auto-injector (7683B series) and a dual-stage cryogenic modulator (LECO, Saint Joseph, MI). Samples were injected in the splitless mode. The cold jet gas was dry N₂ and chilled with liquid N₂. The hot jet temperature offset was 5 °C above the temperature of the secondary GC oven and the inlet temperature was isothermal at 310 °C. Two capillary GC columns were utilized in this GC×GC experiment. First- and second-dimension separations were performed on a Restek Rxi-1ms column (60 m length, 0.25 mm I.D., 0.25 μm df) and a 50% phenyl polysilphenylene-siloxane column (SGE BPX50, 1.2 m length, 0.10 mm I.D., 0.1 μm df), respectively. The temperature program of the main oven was held isothermal at 65 °C (12.5 min) and was then ramped from 65 to 340 °C at 1.25 °C min⁻¹. The second-dimension oven was isothermal at 70 °C (12.5 min) and then ramped from 70 to 345 °C at 1.25 °C min⁻¹. The hot jet pulse width was 0.75 s, while the modulation period between stages was 7.50 s with a 3.00 s cooling period between modulations. FID data were sampled at an acquisition rate of 100 data points per second. The GC×GC was configured for splitless auto-injection, with an inlet temperature of 310 °C, and purge vent opening at 0.5 min. Hydrogen as carrier gas was at a constant flow of 1 mL/min.

GC×GC-HRT analysis: GC×GC – HRT chromatographic analysis was performed on a LECO Pegasus GC×GC – HRT 4D system consisting of an Agilent 7890B GC configured with a LECO LPAL3 split/splitless auto-injector system and a dual-stage cryogenic modulator (LECO, Saint Joseph, MI). Samples were injected in splitless mode. The cold jet gas was dry N₂ chilled with liquid N₂. The hot jet temperature offset was 10 °C above the temperature of the main GC oven and the inlet temperature was isothermal at 310 °C. Two capillary GC columns were utilized in this GC×GC experiment. First- and second-dimension separations were performed on a Restek Rxi-1ms column (60 m length, 0.25 mm I.D., 0.25 μm df) and a SGE BPX-50 column (2 m length, 0.25 mm I.D., 0.25 μm df), respectively. The temperature program of the main oven was held isothermal at 60 °C (5 min) and was then ramped from 60 to 335 °C at 1.5 °C min⁻¹. The hot jet pulse width was 2 s with a modulation period of 10 s. The second-dimension oven was held isothermal at 65 °C (5 min) and was then ramped from 65 to 340 °C at 1.5 °C min⁻¹. The carrier

gas was helium at a flow rate of 1 mL min⁻¹. HR-TOF data were sampled at an acquisition rate of 100 spectra per second (actual data collection rate was 97.2222 spectra per second) in the mass range of 40–600 amu. The ionization method was electron ionization (EI) with an electron energy of -70 V and the extraction frequency was 1.75 kHz.

GC×GC-FID and GC×GC-HRT data were acquired and analyzed using LECO ChromaTOF® software version 5.21, (LECO, Saint Joseph, MI).

Contribution to the field. Hydrocarbons and their fate in Guaymas Basin sediments have been studied previously using laboratory experiments and analytical techniques. Here we provide for the first time an extensive assessment of ~200 semivolatile hydrocarbon compounds in porewaters and sediment cakes from AUV Alvin push cores, and discuss their overall distribution and fate at three distinct hydrothermal areas located the southern axial trough of Guaymas Basin, Cathedral Hill, Aceto Balsamico and Marker 14. These sites are known for their contrasting biogeochemistry and thermal profiles. We couple these data with in-depth GC×GC investigation on the biomarker profile of the most contrasting sediment cores (from Cathedral Hill vs. Marker 14) to provide information on the presence/distribution of predominant indicators of microbial hydrocarbon degradation (e.g., steranes, and hopanes), and their analogs (e.g., diasteranes, C-ring monoaromatic and triaromatic steranes) that could derive from early diagenesis and/or the existing oxidative conditions in Guaymas Basin. We illustrate the changing composition of saturated, polyaromatic, and alkylated polyaromatic hydrocarbons in these deep hydrothermal seep sediment cores from contrasting sites, providing a more detailed understanding of hydrothermal and biological hydrocarbon alteration in this setting.

Reporting summary. Further information on research design is available in the Nature Research Reporting Summary linked to this article.

Data availability

The hydrocarbon, temperature and porewater nutrient profile data used in this study are available through the Biological and Chemical Oceanography Data Management Office (BCO-DMO) at the Woods Hole Oceanographic Institution under project number 474317. Sediment cake hydrocarbon composition can be found at <https://www.bco-dmo.org/dataset/773297/data>⁶⁴ and porewater hydrocarbons at <https://www.bco-dmo.org/dataset/773288/data>⁶⁵. Temperature profile data are found at <https://www.bco-dmo.org/dataset/878936>⁶⁶. Porewater nutrient concentrations are found at <https://www.bco-dmo.org/dataset/773129>⁶⁷.

Received: 18 May 2022; Accepted: 11 October 2022;

Published online: 28 October 2022

References

1. Simoneit, B. R. T. & Lonsdale, P. F. Hydrothermal petroleum in mineralized mounds at the seabed of Guaymas Basin. *Nature* **295**, 198–202 (1982).
2. Simoneit, B. R. T. Hydrothermal petroleum: genesis, migration and deposition in Guaymas Basin, Gulf of California. *Can. J. Earth Sci.* **22**, 1919–1929 (1985).
3. Von Damm, K. L., Edmond, J. M., Measures, C. I. & Grant, B. Chemistry of submarine hydrothermal solutions at Guaymas Basin, Gulf of California. *Geochim. Cosmochim. Acta* **49**, 2221–2237 (1985).
4. Whelan, J. K., Simoneit, B. R. T. & Tarafa, M. C1-C8 hydrocarbons in sediments from Guaymas Basin, Gulf of California—comparison to Peru Margin, Japan Trench and California Borderlands. *Org. Geochem.* **12**, 171–194 (1988).
5. Martens, C. S. Generation of short chain organic acid anions in hydrothermally altered sediments of the Guaymas Basin, Gulf of California. *Appl. Geochem.* **5**, 71–76 (1990).
6. Peter, J. M., Peltonen, P., Scott, S. D., Simoneit, B. R. T. & Kawka, O. E. ¹⁴C ages of hydrothermal petroleum and carbonate in Guaymas Basin, Gulf of California: implications for oil generation, expulsion, and migration. *Geology* **19**, 253–256 (1991).
7. Simoneit, B. R. T., Oros, D. R., Leif, R. N. & Medeiros, P. M. Weathering and biodegradation of hydrothermal petroleum in the north rift of Guaymas Basin, Gulf of California. *Rev. Mex. Cienc. Geol.* **36**, 159–176 (2019).
8. Teske, A. et al. The Guaymas Basin hiking guide to hydrothermal mounds, chimneys and microbial mats: complex seafloor expressions of subsurface hydrothermal circulation. *Front. Microbiol.* **7**, 75 (2016).
9. Pearson, A., Seewald, J. S. & Eglinton, T. I. Bacterial incorporation of relict carbon in the hydrothermal environment of Guaymas Basin. *Geochim. Cosmochim. Acta* **69**, 5477–5486 (2005).
10. McKay, L. et al. Thermal and geochemical influences on microbial biogeography in the hydrothermal sediments of Guaymas Basin, Gulf of California. *Environ. Microbiol. Rep.* **8**, 150–161 (2016).
11. Teske, A. Guaymas Basin, a hydrothermal hydrocarbon seep ecosystem. In *Marine Hydrocarbon Seeps—Microbiology and Biogeochemistry of a Global Marine Habitat* (eds Teske, A. & Carvalho, V.) 43–68 (Springer, 2020).
12. De la Lanza-Espino, G. & Soto, L. A. Sedimentary geochemistry of hydrothermal vents in Guaymas Basin, Gulf of California, Mexico. *Appl. Geochem.* **14**, 499–510 (1999).
13. Rullkötter, J. et al. Organic petrography and extractable hydrocarbons of sediments from the Eastern North Pacific Ocean, Deep Sea Drilling Project LEG63. In *Initial Reports of the Deep-Sea Drilling Project* (eds Curry, J. R. et al.) 837–853 (U.S. Government Printing Office, Washington, DC, 1982).
14. Simoneit, B. R. T. & Bode, G. R. In *Initial Reports of the Deep Sea Drilling Project* (eds Curry, J. R. et al.) 1303–1305 (U.S. Government Printing Office, Washington, DC, 1982).
15. Teske, A. et al. Guaymas basin tectonics and biosphere. In *Proc. International Ocean Discovery Program*, Vol. 385 (International Ocean Discovery Program, College Station, TX) (2021).
16. Ondréas, H., Scalabrin, C., Fouquet, Y. & Godfroy, A. Recent high-resolution mapping of Guaymas hydrothermal fields (Southern Trough). *BSGF—Earth Sci. Bull.* **189**, 6 (2018).
17. Dalzell, C. J. et al. Hydrocarbon transformations in sediments from the Cathedral Hill hydrothermal vent complex at Guaymas Basin, Gulf of California—a chemometric study of shallow seep architecture. *Org. Geochem.* **152**, 104173 (2021).
18. Dowell, F. et al. Microbial communities in methane and short alkane-rich hydrothermal sediments of Guaymas Basin. *Front. Microbiol.* **7**, 17 (2016).
19. Teske, A. et al. Microbial diversity in hydrothermal sediments in the Guaymas Basin: evidence for anaerobic methanotrophic communities. *Appl. Environ. Microbiol.* **68**, 1994–2007 (2002).
20. Edgcomb, V. P., Teske, A. P. & Mara, P. Microbial hydrocarbon degradation in Guaymas Basin—exploring the roles and potential interactions of fungi and sulfate-reducing bacteria. *Front. Microbiol.* **13**, 831828 (2022).
21. Ramirez, G. A. et al. Environmental controls on bacterial, archaeal and fungal community structure in hydrothermal sediments of Guaymas Basin, Gulf of California. *PLoS ONE* **16**, e0256321 (2021).
22. Stout, S. A. Oil spill fingerprinting method for oily matrices used in the Deepwater Horizon NRDA. *Environ. Forensics* **17**, 218–243 (2016).
23. Nelson, R. K. et al. Tracking the weathering of an oil spill with comprehensive two-dimensional gas chromatography. *Environ. Forensics* **7**, 33–44 (2006).
24. Simoneit, B. R. T., Kawka, O. E. & Brault, M. Origin of gases and condensates in the Guaymas Basin hydrothermal system. *Chem. Geol.* **71**, 169–182 (1988).
25. Ventura, G. T., Simoneit, B. R. T., Nelson, R. K. & Reddy, C. M. The composition, origin and fate of complex mixtures in the maltene fractions of hydrothermal petroleum assessed by comprehensive two-dimensional gas chromatography. *Org. Geochem.* **45**, 48–65 (2012).
26. Teske, A. in *Microbial Communities Utilizing Hydrocarbons and Lipids: Members, Metagenomics and Ecophysiology* (ed McGenity, T. J.) 81–111 (Springer Nature Switzerland AG, 2019).
27. Bazyliński, D. A., Farrington, J. W. & Jannasch, H. W. Hydrocarbons in surface sediment from a Guaymas Basin hydrothermal vent site. *Org. Geochem.* **12**, 547–558 (1988).
28. Mackenzie, A. S., Brassell, S. C., Eglinton, G. & Maxwell, J. R. Chemical fossils: the geological fate of steroids. *Science* **217**, 491–504 (1982).
29. Lagostina, L. et al. Interactions between temperature and energy supply drive microbial communities in hydrothermal sediment. *Commun. Biol.* **4**, 1006 (2021).
30. Melendez, I., Grice, K. & Schwark, L. Exceptional preservation of palaeozoic steroids in a diagenetic column. *Sci. Rep.* **3**, 2768 (2013).
31. Calvert, S. E. Origin of diatom-rich, varved sediments from the Gulf of California. *J. Geol.* **74**, 546–565 (1966).
32. Gonzalez-Vila, F. J. In *Composition, Geochemistry and Conversion of Oil Shales* (ed. Snape, C.) 51–69 (Springer, Dordrecht, 1995).
33. Dufourc, E. J. Sterols and membrane dynamics. *J. Chem. Biol.* **1**, 63–77 (2008).
34. Waldbauer, J. R., Newman, D. K. & Summons, R. E. Microaerobic steroid biosynthesis and the molecular fossil record of Archean life. *Proc. Natl. Acad. Sci. USA* **108**, 13409–13414 (2011).
35. Drake, H. et al. Fossilized anaerobic and possibly methanogenesis-fueling fungi identified deep within the Siljan impact structure, Sweden. *Commun. Earth Environ.* **2**, 34 (2021).
36. Edgcomb, V. P. et al. Benthic eukaryotic diversity in the Guaymas Basin, a hydrothermal vent environment. *Proc. Natl. Acad. Sci. USA* **99**, 7658–7662 (2002).
37. Van Andel. Recent marine sediments of Gulf of California. In *Marine Geology of the Gulf of California*, Vol. 3 (eds van Andel T. H. & Shor G.G.) 216–310 (American Association of Petroleum Geologists Memoir, Tulsa).

38. Peter, J. M. & Scott, S. D. Mineralogy, composition, and fluid-inclusion microthermo-metry of seafloor hydrothermal deposits in the southern trough of Guaymas Basin, Gulf of California. *Can. Mineral.* **26**, 657–587 (1988).
39. Wang, J. K. & Seibert, M. Prospects for commercial production of diatoms. *Biotechnol. Biofuels* **10**, 16 (2017).
40. Piloni, R. V., Brunetti, V., Urcelay, R. C., Daga, I. C. & Moyano, E. L. Chemical properties of biosilica and bio-oil derived from fast pyrolysis of *Melosira varians*. *J. Anal. Appl. Pyrolysis* **127**, 402–410 (2017).
41. Bobrovskiy, I. et al. Algal origin of sponge sterane biomarkers negates the oldest evidence for animals in the rock record. *Nat. Ecol. Evol.* **5**, 165–168 (2021).
42. Leif, R. N. & Simoneit, B. R. T. Confined-pyrolysis as an experimental method for hydrothermal organic synthesis. *Orig. Life Evol. Biosph.* **25**, 417–429 (1995).
43. Simoneit, B. R. T., Deamer, D. W. & Kompanichenko, V. Characterization of hydrothermally generated oil from the Uzon caldera, Kamchatka. *Appl. Geochem.* **24**, 303–309 (2009).
44. Atlas, R. M. Petroleum biodegradation and oil spill bioremediation. *Mar. Pollut. Bull.* **31**, 178–182 (1995).
45. Frontera-Suau, R., Bost, F. D., McDonald, T. J. & Morris, P. J. Aerobic biodegradation of hopanes and other biomarkers by crude oil-degrading enrichment cultures. *Environ. Sci. Technol.* **36**, 4585–4592 (2002).
46. Moldowan, J. M. & McCaffrey, M. A. A novel microbial hydrocarbon degradation pathway revealed by hopane demethylation in a petroleum reservoir. *Geochim. Cosmochim. Acta* **59**, 1891–1894 (1995).
47. Oliveira, C. R. et al. Biomarkers in crude oil revealed by comprehensive two-dimensional gas chromatography time-of-flight mass spectrometry: depositional paleoenvironmental proxies. *Org. Geochem.* **46**, 154–164 (2012).
48. Alexander, R., Kagi, R. I., Noble, R. & Volkman, J. K. Identification of some bicyclic alkanes in petroleum. *Org. Geochem.* **6**, 63–72 (1984).
49. Liao, J., Lu, H., Sheng, G., Peng, P. & Hsu, C. S. Monoaromatic, diaromatic, triaromatic, and tetraaromatic hopanes in Kokersite share and their stable carbon isotopic composition. *Energy Fuels* **29**, 3573–3583 (2015).
50. Sessions, A. L. et al. Identification and quantification of polyfunctionalized hopanoids by high temperature gas chromatography–mass spectrometry. *Org. Geochem.* **56**, 120–130 (2013).
51. Siedenburg, G. & Jendrossek, D. Squalene-hopene cyclases. *Appl. Environ. Microbiol.* **77**, 3905–3915 (2011).
52. Volkman, J. K., Alexander, R., Kagi, R. I., Rowland, S. J. & Sheppard, P. N. Biodegradation of aromatic hydrocarbons in crude oils from the Barrow Sub-basin of Western Australia. *Org. Geochem.* **6**, 619–632 (1984).
53. Peters, K. E. & Moldowan, J. M. In *The Biomarker Guide. Interpreting Molecular Fossils in Petroleum and Ancient Sediments* (Prentice-Hall, New York, 1993).
54. Lin, Y.-S. et al. Near-surface heating of young rift sediment causes mass production and discharge of reactive dissolved organic matter. *Sci. Rep.* **7**, 44864 (2017).
55. Elsgaard, L., Isaksen, M. F., Jørgensen, B. B., Alayse, A.-M. & Jannasch, H. W. Microbial sulfate reduction in deep-sea sediments at the Guaymas Basin hydrothermal vent area: influence of temperature and substrates. *Geochim. Cosmochim. Acta* **58**, 3335–3343 (1994).
56. Zhuang, G. C. et al. Generation and utilization of volatile fatty acids and alcohols in hydrothermally altered sediments in the Guaymas Basin, Gulf of California. *Geophys. Res. Lett.* **46**, 2637–2646 (2019).
57. Winkel, M., De Beer, D., Lavik, G., Peplies, J. & Mussmann, M. Close association of active nitrifiers with *Beggiatoa* mats covering deep-sea hydrothermal sediments. *Environ. Microbiol.* **16**, 1612–1626 (2014).
58. Meyer, S. et al. Microbial habitat connectivity across spatial scales and hydrothermal temperature gradients at Guaymas Basin. *Front. Microbiol.* **4**, 207 (2013).
59. Guezennec, J. G. et al. Bacterial community structure from Guaymas Basin, Gulf of California, as determined by analysis of phospholipid ester-linked fatty acids. *J. Mar. Biotechnol.* **4**, 165–175 (1996).
60. Schouten, S., Wakeham, S. G., Hopmans, E. C. & Sinninghe Damste, J. S. Biogeochemical evidence that thermophilic archaea mediate the anaerobic oxidation of methane. *Appl. Environ. Microbiol.* **69**, 1680–1686 (2003).
61. Engelen, B. et al. Microbial communities of hydrothermal Guaymas Basin surficial sediment profiled at 2 millimeter-scale resolution. *Front. Microbiol.* **12**, 710881 (2021).
62. Teske, A. et al. A molecular and physiological survey of a diverse collection of hydrothermal vent *Thermococcus* and *Pyrococcus* isolates. *Extremophiles* **13**, 917–923 (2009).
63. Seitz, K. W. et al. Asgard archaea are capable of anaerobic hydrocarbon cycling. *Nat. Commun.* **10**, 1822 (2019).
64. Edgcomb, V. P. & Teske, A. P. Sediment hydrocarbon concentrations in Alvin pushcore samples from Guaymas Basin hydrothermal vents, RV/Atlantis cruise AT42-05, November 2018. Biological and Chemical Oceanography Data Management Office (BCO-DMO). (Version 1) Version Date 2019-07-15. <https://doi.org/10.26008/1912/bco-dmo.773297.1> (2020).
65. Edgcomb, V. P., Teske, A. P. *Porewater Hydrocarbon Concentrations In Alvin Pushcore Samples from Guaymas Basin Hydrothermal Vents, RV/Atlantis Cruise AT42-05, November 2018. Version 1, Version Date 2019-07-15* (Biological and Chemical Oceanography Data Management Office (BCO-DMO), 2020); <https://doi.org/10.26008/1912/bco-dmo.773288.1>.
66. Teske, A. P. & Edgcomb, V. P. *Temperature Profiles of Hydrothermal Sediments Measured by the Hov Alvin Heat Flow Probe in Guaymas Basin Hydrothermal Vents, R/V Atlantis Cruise AT42-05, November 2018. Version 1, Version Date 2022-08-25* (Biological and Chemical Oceanography Data Management Office (BCO-DMO), 2022); <https://doi.org/10.26008/1912/bco-dmo.878936.1>.
67. Edgcomb, V. & Teske, A. *Porewater Nutrient Concentrations (NO₃+NO₂, NH₄, and PO₄) from Pushcore Samples Collected at Guaymas Basin Hydrothermal Vents via Alvin Dives on RV/Atlantis Cruise AT42-05, November 2018. Version 1, Version Date 2019-07-15* (Biological and Chemical Oceanography Data Management Office (BCO-DMO), 2019); <https://doi.org/10.1575/1912/bco-dmo.773129.1>.

Acknowledgements

We thank the *Alvin* and *Sentry* teams for their expertise and the science crew for collegial support during Guaymas Basin cruise AT42-05. We also thank Dr. Carol Arnosti (University of North Carolina-Chapel Hill) for their helpful comments and suggestions on the manuscript. This work was supported by NSF OCE-1829903 to V.E. and A.T. Mexican sampling permits are noted in the cruise authorization CTC no. 07528, Mexican Department of State, November 9, 2018.

Author contributions

V.E. and A.T. conceived the project and acquired funding. V.E. and P.M. collected samples in Guaymas Basin, and A.T. headed the cruise. P.M. and V.E. handled data curation. R.N. and C.R. conducted GC×GC analyses and R.N. interpreted GC×GC data. P.M. provided biogeochemical context. A.T. wrote the first draft of the manuscript, P.M. and V.E. added it to the manuscript, and all authors contributed to the final writing and editing.

Competing interests

The authors declare no competing interests.

Additional information

Supplementary information The online version contains supplementary material available at <https://doi.org/10.1038/s43247-022-00582-8>.

Correspondence and requests for materials should be addressed to Virginia P. Edgcomb.

Peer review information *Communications Earth & Environment* thanks Meijun Li and the other, anonymous, reviewer(s) for their contribution to the peer review of this work. Primary Handling Editors: Olivier Sulpis, Joe Aslin, Heike Langenberg. Peer reviewer reports are available.

Reprints and permission information is available at <http://www.nature.com/reprints>

Publisher's note Springer Nature remains neutral with regard to jurisdictional claims in published maps and institutional affiliations.



Open Access This article is licensed under a Creative Commons Attribution 4.0 International License, which permits use, sharing, adaptation, distribution and reproduction in any medium or format, as long as you give appropriate credit to the original author(s) and the source, provide a link to the Creative Commons license, and indicate if changes were made. The images or other third party material in this article are included in the article's Creative Commons license, unless indicated otherwise in a credit line to the material. If material is not included in the article's Creative Commons license and your intended use is not permitted by statutory regulation or exceeds the permitted use, you will need to obtain permission directly from the copyright holder. To view a copy of this license, visit <http://creativecommons.org/licenses/by/4.0/>.

© The Author(s) 2022